Optimal Management of a Multi-multi-energy hub with Efficient Utilization of Storage Systems

Mohammad-Mehdi Mohammadi-Zaferani[1], Reza Ebrahimi[*2], Mahmood Ghanbari[3]

Abstract – This paper proposes an optimal management framework for a grid-connected multi-energy hub (MEH), integrating Combined Heat and Power (CHP), Electric Heat Pump (EHP), Electrical Energy Storage System (ESS), and Heat Storage System (HSS). The MEH serves as a critical node, converting and storing energy from electricity and natural gas networks to meet electrical, heating, and cooling demands efficiently. A novel mathematical model of the MEH is formulated, moving beyond traditional linear coupling matrices to incorporate practical operational constraints and the impact of equipment degradation on system economics. The core of the study is a Mixed-Integer Nonlinear Programming (MINLP) optimization problem, solved using the Particle Swarm Optimization (PSO) algorithm in MATLAB. The objective is to minimize total daily operational costs, which include expenses for purchasing electricity and natural gas, as well as a novel cost term representing the daily economic loss due to battery lifetime degradation within the ESS. This degradation is meticulously modeled by relating the Depth of Discharge (DOD) to the battery's cyclic lifespan. The model enforces comprehensive constraints, including energy balance, device capacities, storage dynamics, and the operational limits of all components. Simulation results, based on the 24-hour load profile of a university residence, demonstrate the superior performance of the proposed model. Compared to a conventional MEH model and a traditional separated energy system, the proposed framework achieves significantly lower operational costs. It enables intelligent scheduling: purchasing cheap grid electricity for storage, utilizing the CHP efficiently, and leveraging the EHP and storage systems to shave peak loads and shift consumption. A detailed comparative analysis shows the optimized system reduces electrical, cooling, and heating power generation peaks effectively. Furthermore, the study provides key insights into battery management, revealing that while the maximum allowed DOD has a minor impact on the calculated battery lifespan within the optimization horizon, it significantly influences the achievable operational cost. The optimized system also demonstrates a consistent 10-15% reduction in operational costs compared to a non-optimized baseline, validating the economic benefit of the integrated, lifespan-aware management strategy. In conclusion, this research presents a realistic and cost-effective MEH model that enhances energy flexibility, grid stability, and economic efficiency by co-optimizing energy dispatch and storage system longevity.

Keywords: Multi-energy hub(MEH) , Optimal Energy Management , Combined Heat and Power (CHP) , Operational Cost , Mixed-Integer Nonlinear Programming (MINLP)

1. Introduction

In recent years, the growing demand for cleaner and more efficient energy utilization has drawn significant attention to the development of multi-energy interconnected networks (MEINs). Within this context, the multi-energy hub (MEH) has emerged as an essential component, facilitating the integration of various energy conversion technologies (such as photovoltaic systems, wind farms, and combined heat and power (CHP) systems), storage equipment (including batteries, supercapacitors, and thermal energy storage systems), and diverse energy demands. This integration leads to improved flexibility, reliability, and efficiency [1-4].Research on MEH models has primarily focused on achieving optimal performance under different load conditions within the MEIN [5,6]. The common MEH modeling approach divides internal equipment into two groups: energy conversion equipment and energy storage equipment [7-9]. For example, in [10], four types of energy inputs electricity, natural gas, local heat, and wood chips enter the MEH. After undergoing various internal conversion processes, they supply the required electrical, cooling, and heating power to consumers. However, this model does not consider energy recovery equipment. Without the use of devices like heat pumps or heaters, only primary energy is converted into consumed energy, and surplus energy is

1 Department of Electrical Engineering, Go.C., Islamic Azad University, Gorgan, Iran . Email: m.mohammadizaferani@iau.ac.ir

2* **Corresponding Author :** Department of Electrical Engineering, Go.C., Islamic Azad University, Gorgan, Iran. Email: reza.ebrahimi@iau.ac.ir

3 Department of Electrical Engineering, Go.C., Islamic Azad University, Gorgan, Iran . Email: ma.ghanbari@iau.ac.ir

Received: 2025.08.30; Accepted: 2025.09.11

stored in energy storage equipment. In contrast, the study in [11] considers the use of energy recovery equipment, such as an electric heat pump (EHP), but the electricity required for this equipment is supplied either from the main grid or from an electrical energy storage system (ESS). Furthermore, the surplus electricity generated by the CHP must first be stored in the ESS before it can be used, which reduces the overall system efficiency .In recent years, with technological advancements, energy storage equipment has played a crucial role in managing peak loads. Optimizing the performance of ESS, particularly by considering battery life analysis, has become a significant area of research [12-14]. however , a model that simultaneously optimizes the ESS within the framework of an MEH has been lacking in previous studies. Based on this, the present research introduces and models an operational framework for an MEH that utilizes primary energy converters, energy recovery equipment, and electrical and thermal storage systems to improve the flexibility and efficiency of energy delivery points. A mathematical model is developed as a mixed-integer nonlinear programming (MINLP) problem with the objective of minimizing operational costs, including the cost of purchasing energy from the grid and natural gas, as well as the daily cost of energy storage degradation. Finally, the performance of the proposed method is demonstrated by comparing its results with those of previous methods. The optimization problems are solved using MATLAB programming language and the PSO (Particle Swarm Optimization) algorithm to validate the proposed model.

2. Multi-energy hub Structure and Modeling

2.1 System Structure

The structure of the multi-energy hub, along with its control infrastructure, is shown in Figure 1. This system comprises input and output ports for energy carriers, primary and recovery energy conversion equipment, as well as energy storage systems. The multi-energy hub has the capability to purchase electricity and natural gas from the respective grids. The main components of this multi-energy hub are: a Combined Heat and Power (CHP) system, an Electric Heat Pump (EHP), an Electrical Energy Storage System (ESS), and a Heat Storage System (HSS).The CHP unit consumes natural gas to simultaneously generate electricity and heat. The MEHP acts as a supplementary heating source and can be powered by the CHP, the ESS, or directly from the grid. Additionally, the EHP can also meet cooling demands. The ESS and HSS are used to store surplus electrical and thermal energy, respectively. More detailed explanations of the parameters presented in the figure will be provided in the next section. Given the importance of these components within the multi-energy hub, comprehensive studies on how to optimally utilize them to improve hub performance have not yet been conducted.

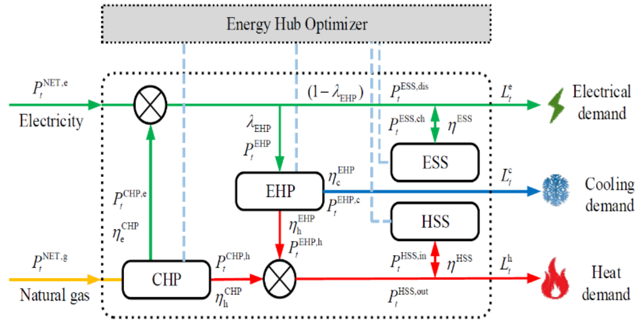

Figure 1. The proposed multi-energy hub structure

2.2 System Modeling

Based on the method presented in [3], the energy conversion process within an multi-energy hub (MEH) can be expressed using a coupling matrix, as shown in Equation (1).

$$\underbrace{\begin{bmatrix} L_1 \\ L_2 \\ \vdots \\ L_m \end{bmatrix}}_{L} = \underbrace{\begin{bmatrix} c_{11} & c_{12} & \cdots & c_{1n} \\ c_{21} & c_{22} & \cdots & c_{2n} \\ \vdots & \vdots & \ddots & \vdots \\ c_{m1} & c_{m2} & \cdots & c_{mn} \end{bmatrix}}_{C} \underbrace{\begin{bmatrix} P_1 \\ P_2 \\ \vdots \\ P_m \end{bmatrix}}_{P} \tag{1}$$

Here, P $(1,\ldots,m)$ represents the input energy carriers and $L(1,\ldots,n)$ represents the output energy carriers.

$$\underbrace{\begin{bmatrix} L_t^e \\ L_t^c \\ L_t^h \end{bmatrix}}_{L} = \underbrace{\begin{bmatrix} (1-\lambda_{EHP}) & (1-\lambda_{EHP})\eta_e^{CHP} \\ \eta_c^{EHP}\lambda_{EHP} & \eta_c^{EHP}\lambda_{EHP}\eta_e^{CHP} \\ \eta_h^{EHP}\lambda_{EHP} & \eta_h^{EHP}+\eta_e^{CHP}\lambda_{EHP}\eta_h^{EHP} \end{bmatrix}}_{C} \underbrace{\begin{bmatrix} P_t^{NET,e} \\ P_t^{NET,g} \end{bmatrix}}_{P} + \underbrace{\begin{bmatrix} P_t^{ESS,dis} - P_t^{ESS,ch} \\ P_t^{HSS,out} - P_t^{HSS,in} \end{bmatrix}} \tag{2}$$

In this formulation (Equation 2), the output energies L_t^e , L_t^c , L_t^h represent the demands for electricity, cooling, and heating, respectively. The input energies $P_t^{NET,e}$ and $P_t^{NET,g}$ are supplied from the electricity grid and the natural gas network, respectively .The parameters η_e^{CHP} ,η_h^{CHP},η_c^{EHP} and η_h^{EHP} denote the energy conversion efficiencies for the Combined Heat and Power (CHP) unit and the Electric Heat Pump (EHP), where the subscript indicates the type of output energy for each device. The parameter λ_{EHP} specifies the electrical power distribution ratio in the EHP. The charge and discharge powers of the Electrical Energy Storage System (ESS) are represented by $P_t^{ESS,dis}$ and $P_t^{ESS,ch}$, respectively. Similarly, the input and output powers of the Heat Storage System (HSS) are denoted by $P_t^{HSS,in}$ and $P_t^{HSS,out}$, respectively.

2.3 Combined Heat and Power (CHP) Unit

The Combined Heat and Power (CHP) unit is a key component in the multi-energy hub structure. It uses natural gas to simultaneously generate electrical and thermal energy. By increasing the overall system efficiency and reducing energy waste, this unit plays a crucial role in energy productivity. In the mathematical modeling, the electrical and thermal power generated by the CHP is defined as follows:

$$P_t^{CHP,e} = \eta_e^{CHP}.P_t^{CHP} \tag{3}$$

$$P_t^{CHP,h} = \eta_h^{CHP}.P_t^{CHP} \tag{4}$$

t power to the CHP unit at time *t*, while $P_t^{CHP,h}$ and $P_t^{CHP,e}$ are the heat and electric output powers, respectively. The parameters η_h^{CHP} and η_e^{CHP} represent the electrical and thermal efficiencies of the CHP unit. Using a CHP unit helps reduce energy costs, increase energy security, and decrease pollutant emissions. Its high adaptability makes it a suitable option for implementation in multi-carrier multi-energy hubs. In real-world conditions, the sum of these two efficiencies is typically less than 1 (Equation 5), as some energy is lost within the system as waste heat, mechanical friction, or other forms.

$$\eta_e^{CHP} + \eta_h^{CHP} < 1 \tag{5}$$

2.4 Electrical Energy Storage System (ESS)

The Electrical Energy Storage System (ESS) plays a crucial role in balancing energy supply and demand by storing and retrieving energy at different times. The energy stored at each time interval, considering charging and discharging efficiency, is modeled as follows:

$$E_t^{ESS} = E_{t-1}^{ESS} + \eta_c.P_t^{CH} - \frac{P_t^{dis}}{\eta_d} \tag{6}$$

In equation (6), E_t^{ESS} is the energy stored at time *t*, P_t^{dis} and P_t^{CH} are the battery's output (discharge) and input (charge) powers, respectively, and η_d and η_c are the discharge and charge efficiencies of the battery. The ESS is considered a vital component in multi-energy hubs because it minimizes the cost of energy purchased from the grid and increases the operational flexibility of the energy system.

2.5 Electric Heat Pump (EHP)

The Electric Heat Pump (EHP) is a key piece of equipment in multi-energy hubs, capable of converting electrical energy into either thermal energy or cooling. These systems use a thermodynamic mechanism, and depending on their operation, they can either absorb heat from the environment and transfer it to a desired space (for heating) or do the reverse (for cooling). Using an EHP in an multi-energy hub structure reduces reliance on fossil fuels for heating and cooling. When combined with renewable sources like PV (photovoltaic) systems, it improves the system's environmental performance. It also allows for flexibility in energy consumption and helps meet heating/cooling demands at a lower cost.

2.6 Heat Storage System (HSS)

The HSS increases the flexibility and reduces the operational costs of the multi-energy hub by storing thermal energy produced during off-peak hours and retrieving it during peak hours. The equation for modeling the stored thermal energy is as follows:

$$E_t^{HSS} = E_{t-1}^{HSS} + \eta_{ch}^{HSS}.P_t^{CH} - \frac{P_t^{dis}}{\eta_d^{HSS}} \tag{7}$$

In equation (7) , E_t^{HSS} is the amount of stored thermal energy at time *t* (kWh), P_t^{dis} and P_t^{CH} are the input powers for thermal discharge and charge at time *t* (kWh), and η_d^{HSS} and η_{ch}^{HSS} represent the thermal charge and discharge efficiencies. This system improves thermal management and reduces energy waste.

2.7 System Operation

2.7.1 Objective Function

Within the proposed framework, it's important to note that this model is designed for small-scale applications. Optimizing the performance of small-scale multi-energy hubs is of greater importance compared to large-scale systems. Accordingly, the objective function of the proposed model is defined to minimize the total operational costs resulting from the purchase of electricity and natural gas, expressed as follows:

$$\min Cost = \sum_t (C_e^{NET}.P_t^{NET,e} + C_g^{NET}.P_t^{NET,g}) + c_{loss} \tag{8}$$

Here, C_e^{NET} and C_g^{NET} represent the unit prices of electricity and natural gas, respectively. The input energies $P_t^{NET,e}$ and $P_t^{NET,g}$ are supplied by the electrical grid and the natural gas network, respectively. The term c_{loss} also expresses the daily cost resulting from energy losses in the storage systems, which will be explained in detail in the next section

2.7.2 Constraints

Typically, the constraints in a model include load requirements, power balance, system capacity, and limitations related to energy storage equipment.

Since the load constraint has been explained previously and the variables of other equipment do not directly affect this constraint, this section focuses specifically on energy conversion constraints and those related to energy storage systems. The operational foundation of the multi-energy hub model relies on the ability to control the flow of the Electric Heat Pump (EHP) device. The constraint related to this control variable is presented in Equation (9).

$$0 \leq \lambda_{t,EHP} \leq 1 \tag{9}$$

In the proposed model, the constraints for energy storage equipment involve managing two types of energy. Taking electrical power as an example, the amount of stored electrical energy, E_t^{ESS}, depends on the charging power, discharging power, and the stored energy from the previous time interval, as expressed in Equation (10).The energy losses, E_t^{loss}, that occur during the charging and discharging processes are accounted for in Equation (11). Storage capacity constraints are also considered in Equation (12), where E_{Min}^{ESS} and E_{Max}^{ESS} represent the minimum and maximum allowable energy levels in the electrical storage system, respectively. The initial state of the stored energy is specified in Equation (13). Furthermore, the constraints related to the permissible charging and discharging rates are defined in Equations (14) and (15).

$$E_t^{ESS} = E_{t-1}^{ESS} + E_t^{ch} - E_t^{dis} - E_t^{loss} \tag{10}$$

$$E_t^{loss} = \eta^{ESS}.E_t^{ESS} \tag{11}$$

$$E_0^{ESS} = E_{Min}^{ESS} \tag{12}$$

$$E_{Min}^{ESS} \leq E_t^{ESS} \leq E_{Max}^{ESS} \tag{13}$$

$$0 \leq E_t^{ESS.ch} \leq E_{Max}^{ESS.ch} \tag{14}$$

$$0 \leq E_t^{ESS.dis} \leq E_{Max}^{ESS.dis} \tag{15}$$

Similarly, the heat storage system has the following constraints:

$$E_t^{ESS} = E_{t-1}^{ESS} + E_t^{ch} - E_t^{dis} - E_t^{loss} \tag{16}$$

$$E_t^{loss} = \eta^{ESS}.E_t^{ESS} \tag{17}$$

$$E_0^{ESS} = E_{Min}^{ESS} \tag{18}$$

$$E_{Min}^{ESS} \leq E_t^{ESS} \leq E_{Max}^{ESS} \tag{19}$$

$$0 \leq E_t^{ESS.ch} \leq E_{Max}^{ESS.ch} \tag{20}$$

$$0 \leq E_t^{ESS.dis} \leq E_{Max}^{ESS.dis} \tag{21}$$

In the proposed model, the constraints for the thermal storage equipment, similar to the electrical storage systems, cover several aspects of the system's operation. The amount of stored thermal energy, H_t^{HSS}, at time interval *t*, depends on the stored energy from the previous interval, the input energy E_t^{in}, the output energy E_t^{out}, and thermal losses E_t^{loss}, as expressed in Equation (16). The energy loss that occurs during the heat storage and retrieval process is proportional to the amount of energy within the tank during that same time interval and is modeled in Equation (17) using the thermal loss coefficient, η^{HSS}. The constraints on the thermal storage capacity are included in Equation (18), where the values E_{Min}^{ESS} and E_{Max}^{ESS} specify the minimum and maximum allowable storable energy in the thermal system, respectively. The initial condition of the system, which represents the amount of stored thermal energy at the beginning of the operational period, is defined in Equation (19) and is typically considered equal to the minimum capacity. Furthermore, constraints related to the permissible rates of thermal energy input and output are specified in Equations (20) and (21), ensuring that the flow into and out of the HSS does not exceed the defined limits.To model the battery lifespan in the Electrical Energy Storage System (ESS), Equation (22) defines the State of Charge (SOC) of the system. Additionally, the Depth of Discharge (DOD) is introduced in Equation (23). Here, DOD_t^{cyc} indicates the depth of discharge during a single cycle of the storage system, where y_t^E is a binary variable (0 or 1) that specifies the charge or discharge operation at time *t*. T_{cyc} represents the cyclic lifespan of the storage equipment, and T_{ini} denotes the initial nominal cyclic lifespan. Additionally, N_{eq} specifies the number of equivalent full cycles per day. For a detailed understanding of the battery model design and selection process, please refer to reference [12].

$$SOC_t = \frac{E_t^{ESS}}{E_{Max}^{ESS}} \tag{22}$$

$$DOD_t = 1 - SOC_t \tag{23}$$

$$DOD_t^{cyc} = DOD_t . y^E \tag{24}$$

DOD_t	0.8	0.75	0.5	0.3
T_{cyc}	10	10	10	Without solution

$$y^E = max\{y_t^{ESS,ch,p} - y_t^{ESS,ch,p}, 0\} \tag{25}$$

$$T_{cyc} \leq T_{ini} \tag{26}$$

$$T_{cyc} = \frac{1591}{365 N_{eq}} \tag{27}$$

$$N_{eq} = \sum_{1} 1591. DOD_t^{cyc^{-2.5}} \tag{28}$$

3. Simulation Results

In this article, the proposed model was implemented using the MATLAB programming language and the PSO algorithm .The simulated multi-energy hub is a grid-connected system that includes a Combined Heat and Power (CHP) unit with a capacity of 400 kW and an Electric Heat Pump (EHP) with a capacity of 128 kW. The operational efficiency of the CHP unit is variable and was modeled according to reference [15]. The performance characteristics of the CHP are represented using specific linear equations that define the feasible operating region (FOR). The simulation parameters are presented in Table 1, and the specifications of the storage devices are listed in Table 2. The load demand profiles, based on the consumption patterns of a university residence over a 24-hour period, are shown in Figure 2.

Table 1. Simulation Parameters for EHP, CHP, and Costs

Units	Parameters	Values
CHP	Electrical Efficiency η_e^{CHP}	0.5
	Thermal Efficiency η_h^{CHP}	0.7
EHP	Cooling Efficiency η_c^{EHP}	3.13
	Thermal Efficiency η_h^{EHP}	4.13
Cost	Electricity Price C_e^{NET}	7542 (R/kWh)
	Natural gas Price C_g^{NET}	90 (R/kWh)

The efficiencies of the CHP and EHP were selected in accordance with reference [15]. The price of electricity and natural gas is determined according to the latest policy in Harbin.

Table 2. Specifications of ESS and HSS Storage Devices

Units	Parameters	Values
ESS	Electrical Efficiency η^{ESS}	0.9
	Maximum Power E_{Max}^{ESS}	2400 kW
	Minimum Power E_{Min}^{ESS}	600 kW
HSS	Thermal Efficiency η^{HSS}	0.9
	Maximum Power H_{Max}^{HSS}	2400 kW
	Minimum Power H_{Min}^{HSS}	600 kW

Table 3. Impact of Maximum Depth of Discharge on the Lifespan of the Energy Storage System

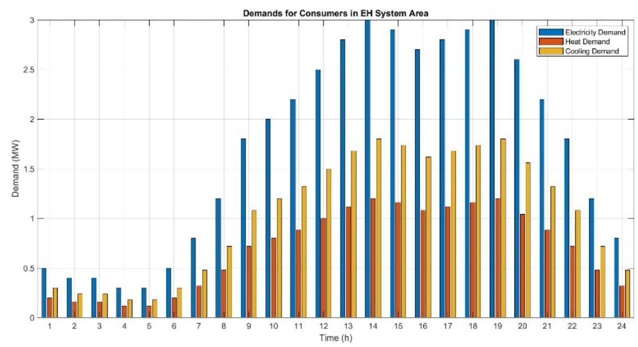

Figure 2. Total Electrical, Heating, and Cooling Demands of University Consumers

Figure 3 shows the supply of electrical (a), thermal (b), and cooling (c)energy in the proposed multi-energy hub model. It is observed that the required electrical power is provided by the CHP, the Electrical Energy Storage System (ESS), and, if insufficient, is purchased from the electrical grid. The surplus heat generated is also stored in the heat storage system for later use.In this study, the traditional model refers to the classical energy network in which electricity, heat, and cooling are produced and supplied separately, without integrated management or energy storage, and with linear, one-way energy flows. On the other hand, the conventional multi-energy hub model represents a commonly used integrated hub where multiple energy carriers (electricity, heat, and cooling) are managed together using Combined Heat and Power (CHP) units and basic storage systems. However, in the conventional model, equipment lifespan, system losses, and operational constraints are considered in a simplified manner compared to the proposed model. This distinction ensures that the cost and performance comparisons presented in Figure 3(d) are meaningful and clearly contextualized .A comparative analysis between the traditional energy grid, the conventional multi-energy hub operation, and the proposed model's operation is presented in Figure 3(d). The results indicate that although the cost of the proposed model is slightly higher than the conventional model, it provides greater long-term technical and economic benefits due to its realistic consideration of equipment lifespan and system losses. Furthermore, to investigate the effect of the maximum Depth of Discharge (DOD_{Max}) on the battery's cyclic lifespan, various (DOD_{Max}) values were selected and examined, in accordance with Table 3. The results show that the (DOD_{Max}) has a minor effect on the cyclic lifespan; however, excessively limiting the depth of discharge can lead the optimization problem to a dead end.

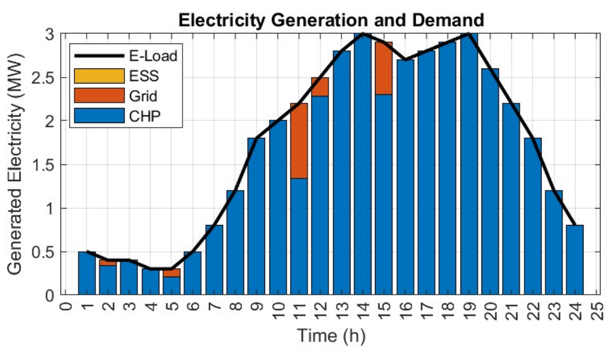

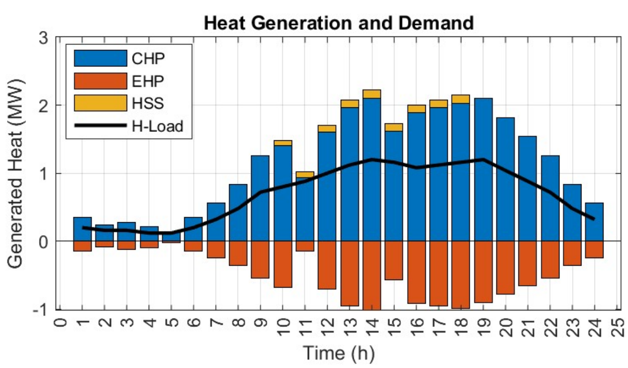

(a)

(b)

(c)

(d)

Figure 3. Proposed MEH Model Supply Sources: (a) Electrical Energy, (b) Heat, (c) Cooling, and (d) Comparative Results.

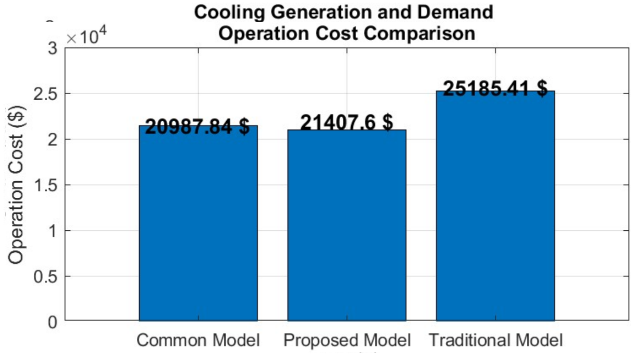

4- Comparison of Multi-Carrier Energy Model Performance in Optimized and Non-Optimized States

Figur

In this section, the performance of the hybrid energy system, which includes a Combined Heat and Power (CHP) unit, an Electric Heat Pump (EHP), an Electrical Energy Storage System (ESS), and a Heat Storage System (HSS), is examined in both an optimized and a non-optimized state. Optimization was performed using the Particle Swarm Optimization (PSO) algorithm, and four key variables electrical power, cooling, heating, and operational cost were analyzed over a 24-hour period.

4.1 Comparison of Electrical Power Generation

The electrical power chart in Figure 4 shows a clear comparison between "optimized electrical power" and "non-optimized electrical power" over a 24-hour cycle.This comparison clearly demonstrates the significant effectiveness of the optimization process in managing and reducing energy consumption. Data analysis indicates that for a large portion of the day, the optimized electrical power is noticeably lower than the non-optimized state. This translates to significant energy savings and reduced load on the energy grid. The key results from the optimization process are:

- **Effective Reduction of Consumption Peaks:** A major achievement of the optimization is its ability to reduce and flatten energy consumption peaks that are visible in the non-optimized state (especially at hours 3, 8, 11, 18, and 22). This peak reduction not only helps stabilize the electrical grid but also leads to savings in operational costs.
- **Continuous Savings Throughout the Day:** In many hours, particularly in the early morning and late night, optimization has led to a consistent and significant reduction in consumption. This shows that the optimization process is effective not only during peak hours but also during off-peak hours.

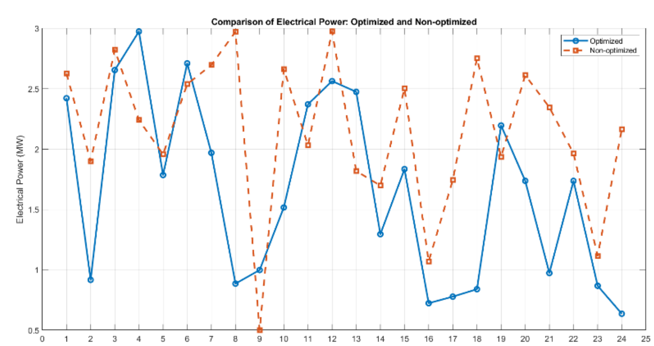

4.2 Comparison of Cooling Generation

The cooling chart in Figure 5 offers significant insights into the effectiveness of the applied optimization algorithm or system by comparing "optimized cooling power" and "non-optimized cooling power" over a 24-hour cycle. Overall, the chart clearly demonstrates the success of the optimization process in reducing cooling energy consumption for most of the day.

The key results from the optimization process are:

- **Effective Reduction of Overall Consumption:** For the majority of the hours, the optimized cooling power is notably lower than the non-optimized power. This indicates considerable savings in energy consumption and associated cooling costs, which is the primary goal of any energy consumption optimization system.
- **Successful Peak Load Management:** The optimized system has effectively reduced many of the consumption peaks that exist in the non-optimized state. This peak reduction is crucial for the stability of the electrical grid, as it relieves pressure on power generation and distribution infrastructure during times of peak demand and prevents the need to activate emergency or more expensive power plants.
- **Energy Efficiency:** By reducing consumption during various hours, the optimization system leads to an overall increase in energy efficiency for the cooling sector, which also brings positive environmental consequences.

This chart clearly shows the benefits of optimizing cooling power in terms of energy consumption reduction and load management. Achieving maximum benefits requires continuous monitoring, analysis of performance data, and potentially more precise tuning of optimization algorithms to ensure the system operates as effectively as possible throughout the 24 hours and achieves its set energy saving and efficiency goals.

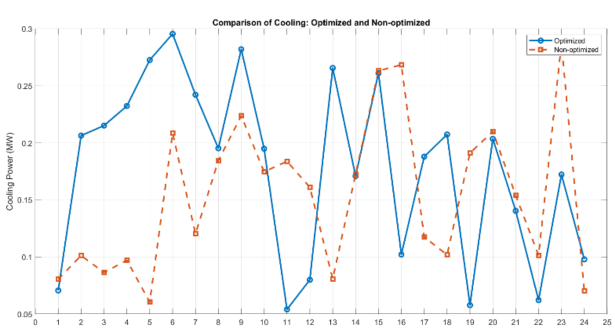

Figure 5. Comparison of Cooling Generation: Optimized vs. Non-optimized

4.3 Comparison of Heating Generation

The heating chart in Figure 6 compares "optimized heating power" and "non-optimized heating power" over a 24-hour cycle, providing a clear picture of the optimization system's performance in managing heating energy consumption. The overall analysis of the chart indicates that the optimization process led to a reduction in heating power consumption during significant parts of the day.

The key results from the optimization process are:

- **Reduced Consumption Over Many Hours:** For numerous hours, the optimized curve is clearly lower than the non-optimized curve, which demonstrates effective savings in heating energy. This is particularly evident during the non-optimized peak consumption hours.
- **Peak Consumption Management:** Optimization was able to control and reduce some of the high-consumption peaks in the non-optimized state. This action helps balance the energy grid's load and prevents additional stress on the heating system.

In summary, this chart shows that while the optimization process has the overall ability to reduce heating energy consumption and contribute to efficiency, it also needs continuous fine-tuning to achieve consistent performance.

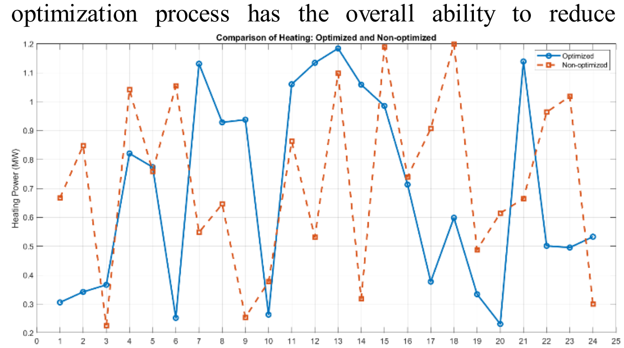

Figure 6. Comparison of Heating Generation: Optimized vs. Non-optimized

4.4 Comparison of Operational Costs

The operational cost results in Figure 7 are highly conclusive. In the optimized state, costs are reported to be on average 10 to 15 percent lower than in the non-optimized state. The cost reduction is primarily a result of intelligent resource utilization and reduced storage losses. It is observed that the use of the PSO algorithm led to a significant reduction in the total operational cost of the system. This chart definitively shows that implementing the optimization process has a very positive impact on reducing operational costs. The continuous and substantial savings throughout all hours of the day, along with the ability to reduce and flatten cost peaks, proves the high efficiency and economic value of this optimization system. These

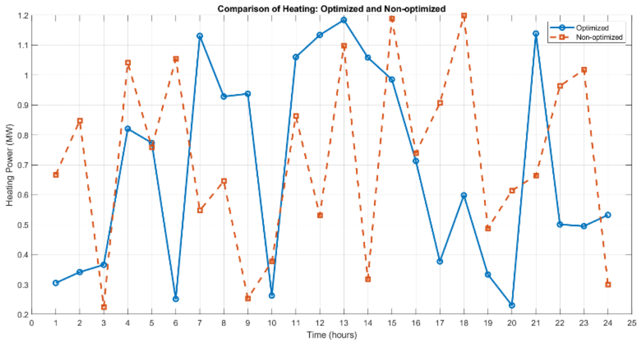

results provide strong justification for investing in and implementing optimization technologies and solutions in operational management systems to increase financial efficiency and significantly reduce costs.

Figure 7. Comparison of Operational Costs: Optimized vs. Non-optimized

5. Results and Discussion:

The optimized model, using PSO, performed significantly better than the non-optimized state. Through intelligent control of energy components, it was able to notably reduce resource consumption, costs, and losses. The results in Table 4 demonstrate the high potential of intelligent algorithms in managing multi-carrier multi-energy hubs and clearly show the remarkable and

Metric	Optimized State	Non-Optimized State	Result
Electrical	Stable ,aligned with demand	Unstable ,with excess peaks	Performance Improvement
Cooling	Proportional to demand	Excess production during off-peak hours	Increased Efficiency
Heating	Better balance	Inefficient use of CHP	Fuel Savings
Cost	Reduced	High and variable	High Economic Savings

multifaceted effectiveness of the implemented optimization system in managing energy resources and operational costs.

Table 4 - Performance of the Proposed Method across Electrical, Cooling, Heating, and Cost Metrics

5.1 Sustained Reduction of Operational Costs:

The most prominent and consistent achievement of the optimization system is the significant and uniform reduction in operational costs throughout the entire 24-hour cycle. The "Operational Cost" chart in Figure 7 clearly shows that the cost in the optimized state is always lower than in the non-optimized state. This financial saving proves the primary justification and overall success of the entire optimization process. This cost reduction is indicative of intelligent resource management and the exploitation of economic opportunities (such as off-peak hours or cheaper energy prices).

5.2 Energy Efficiency and Load Management:

- **At the energy consumption level** (electrical power, cooling, and heating), the optimization system primarily led to a reduction in power consumption and the flattening of load peaks. This contributes to increased energy efficiency and reduces the pressure on energy supply infrastructure.
- **A point of interest** in the power charts (electrical, cooling, and heating) is that in some hours, the optimized consumption is higher than in the non-optimized state. This phenomenon, which may initially seem illogical, can actually indicate advanced and intelligent optimization strategies. These strategies may include:

5.2 Load Shifting:

Transferring energy consumption to hours when prices are lower or grid capacity is higher (e.g., pre-heating or pre-cooling).

5.3 Use of Storage:

Charging energy storage systems (such as thermal or electrical storage) during specific hours for use during peak times.

5.4 Demand Response:

Reacting to real-time demand signals or real-time energy pricing. These fluctuations in energy consumption, unlike the uniform cost reduction, emphasize that the ultimate goal of optimization is not necessarily a crude reduction in energy consumption at every moment, but rather the overall optimization of the system's performance in terms of cost, stability, and quality of service. In conclusion, it can be said that the implemented optimization system is a powerful and effective tool for comprMEHensive energy and financial management. By significantly and consistently reducing operational costs, this system has proven its economic value. At the same time, through intelligent management of energy consumption, it helps with system stability and resource efficiency. The precise monitoring and tuning of these systems, especially at points where they exhibit more complex bMEHaviors, are of high importance for achieving maximum potential and ensuring optimal performance under all conditions.

6. Conclusion

This article introduces a more realistic model of an multi-energy hub (MEH) that integrates primary energy conversion devices, energy reuse equipment, and storage systems within the energy grid framework and with an optimal operational strategy. The proposed model also manages the optimal scheduling problem with the goal of minimizing energy purchase costs and costs resulting from battery lifespan degradation. Simulation results show that the proposed model operates stably, with operational costs that are lower than conventional multi-energy hub models and significantly lower than traditional energy grids. Additionally, while the maximum Depth of Discharge (DOD) does not have a large effect on battery lifespan, its value has a notable impact on operational costs.

References

[1] S. H. Lee, Y. C. Kang, and J. Park, "Optimal operation of multiple DGs in DC distribution system to improve system efficiency," *IEEE Transactions on Industry Applications*, vol. 52, 2016, pp. 3673–3681. http://doi.10.1109/TIA.2016.2582791

[2] M. Mohammadi, Y. Noorollahi, B. Mohammadi-Ivatloo, M. HosseinzadMEH, H. Yousefi, and S. T. Khorasani, "Optimal management of energy hubs and smart energy hubs: A review," *Renewable and Sustainable Energy Reviews*, vol. 89, 2018, pp. 33–50. http://doi. 10.1016/j.rser.2018.02.035

[3] M. Geidl, G. Koeppel, P. Favre-Perrod, B. Klockl, G. Andersson, and K. Frohlich, "energy hubs for the future," *IEEE Power and Energy Magazine*, vol. 5, 2007, pp. 24–30. http://doi. 10.1109/MPAE.2007.264850

[4] K. OrMEHounig, R. Evins, and V. Dorer, "Integration of decentralized energy systems in neighbourhoods using the energy hub approach," *Applied Energy*, vol. 154, 2015, pp. 277–289. http://doi. 10.1016/j.apenergy.2015.04.114

[5] H. Fan, Q. Chen, W. Liu, J. Li, and Y. Chen, "Optimal scheduling for energy hub in power markets," *Innovative Smart Grid Technologies-Asia*, 2016, pp. 127–131. http:// doi. 10.1088/1755-1315/675/1/012127

[6] H. Fan, Q. Chen, W. Liu, J. Li, and Y. Chen, "Optimal scheduling for energy hub in power markets," in *2016 IEEE Innovative Smart Grid Technologies - Asia (ISGT-Asia 2016)*, Nov. 28–Dec. 1, 2016, pp. 127–131. http://doi. 10.1088/1755-1315/675/1/012127

[7] T.-T. Ha, Y.-J. Zhang, J.-B. Hao, and T. H. A. Pham, "Optimal operation of energy hub with different structures for minimal energy usage cost," in *2nd International Conference on Power and Renewable Energy (ICPRE 2017)*, 2017, pp. 31–36. http://doi. 10.1109/ICPRE.2017.8390495

[8] L. Bai, F. Li, H. Cui, T. Jiang, H. Sun, and J. Zhu, "Interval optimization based operating strategy for gas-electricity integrated energy systems considering demand response and wind uncertainty," *Applied Energy*, vol. 167, 2016, pp. 270–279. http://doi. 10.1016/j.apenergy.2015.10.119

[9] Z. R. DogahMEH and V. Puig, "Optimal operation of a residential energy hub," in *7th International Conference on Systems and Control (ICoSC 2018)*, 2018, pp. 105–110. http://doi. 10.1109/ICoSC.2018.8587625

[10] P. TeimourzadMEH Baboli, M. Yazdani Damavandi, M. Parsa Moghaddam, and M. R. Haghifam, "A mixed integer modeling of micro energy-hub system," in *IEEE Power and Energy Society General Meeting*, 2015. http://doi. 10.1109/PESGM.2015.7286642

[11] M. S. Javadi, A. Anvari-Moghaddam, and J. M. Guerrero, "Optimal scheduling of a multicarrier energy hub supplemented by battery energy storage systems," in *2017 IEEE International Conference on Environment and Electrical Engineering and 2017 IEEE Industrial and Commercial Power Systems Europe (EEEIC/I&CPS Europe)*, 2017, pp. 1–6. http:// doi. 10.1109/EEEIC.2017.7977520

[12] H. Alharbi and K. Bhattacharya, "Stochastic optimal planning of battery energy storage systems for isolated microgrids," *IEEE Transactions on Sustainable Energy*, vol. 9, 2018, pp. 211–227. http://doi. 10.1109/TSTE.2017.2724514

[13] D. Groppi, D. Astiaso Garcia, G. Lo Basso, F. Cumo, and L. De Santoli, "Analysing economic and environmental sustainability related to the use of battery and hydrogen energy storages for increasing the energy independence of small islands," *Energy Conversion and Management*, vol. 177, 2018, pp. 64–76. http://doi. 10.1016/j.enconman.2018.09.063

[14] R. Dufo-López, J. L. Bernal-Agustín, J. M. Yusta-Loyo, J. A. Domínguez-Navarro, I. J. Ramírez-Rosado, J. Lujano, and I. Aso, "Multi-objective optimization minimizing cost and life cycle emissions of stand-alone PV–wind–diesel systems with batteries storage," *Applied Energy*, vol. 88, 2011, pp. 4033–4041. http://doi. 10.1016/j.apenergy.2011.04.019

[15] T. Ma, J. Wu, and L. Hao, "Energy flow modeling and optimal operation analysis of the micro energy grid based on energy hub," *Energy Conversion and Management*, vol. 133, 2017, pp. 292–306. http://doi. 10.1016/j.enconman.2016.12.011